

# Synthesis, structure, and magnetic properties of $\text{Ba}_2\text{Cu}_2\text{US}_5$

Hui-yi Zeng, Jiyong Yao, James A. Ibers\*

Department of Chemistry, Northwestern University, 2145 Sheridan Road, Evanston, IL 60208-3113, USA

Received 27 August 2007; received in revised form 24 December 2007; accepted 27 December 2007

Available online 31 December 2007

## Abstract

The alkaline-earth uranium chalcogenide  $\text{Ba}_2\text{Cu}_2\text{US}_5$  was obtained in a two-step reaction from  $\text{BaS}$ ,  $\text{Cu}_2\text{S}$ , and  $\text{US}_2$ .  $\text{Ba}_2\text{Cu}_2\text{US}_5$  crystallizes in a new structure type in space group  $C2/m$  of the monoclinic system with two formula units in a cell of dimensions  $a = 13.606(3) \text{ \AA}$ ,  $b = 4.0825(8) \text{ \AA}$ ,  $c = 9.3217(19) \text{ \AA}$ , and  $\beta = 116.32(3)^\circ$  (153 K). The structure consists of  ${}^\infty_2[\text{Cu}_2\text{US}_5^{4-}]$  layers separated by Ba atoms in bicapped trigonal-prismatic coordination. The two-dimensional  ${}^\infty_2[\text{Cu}_2\text{US}_5^{4-}]$  layer is built from  $\text{US}_6$  octahedra and  $\text{CuS}_4$  tetrahedra. The connectivity of the  $MS_n$  polyhedra within the layer in the [001] direction is *oct tet tet oct tet tet*. A  $\mu_{\text{eff}}$  value of  $2.69(2) \mu_{\text{B}}/\text{U}$  was obtained from the magnetic susceptibility data. No magnetic transition was observed for  $\text{Ba}_2\text{Cu}_2\text{US}_5$  down to 2 K.

© 2008 Elsevier Inc. All rights reserved.

**Keywords:** Uranium; Alkaline-earth; Crystal structure; Magnetism; Synthesis; Layered structure

## 1. Introduction

Interest in actinide chalcogenides stems not only from their varied structures but also from their magnetic and electrical properties that are associated with the more diffuse  $5f$  orbitals vs. the  $4f$  orbitals of the rare-earths. Many alkali-metal ternary and quaternary actinide (poly)chalcogenides have been synthesized [1–12] with the use of the reactive flux method [13]. However, only a few ternary and no quaternary alkaline-earth actinide chalcogenides have been reported [6,14–20]. Here we present the synthesis, structure, and magnetic properties of  $\text{Ba}_2\text{Cu}_2\text{US}_5$ , the first example of a quaternary alkaline-earth actinide chalcogenide.

## 2. Experimental

### 2.1. Syntheses

The following reagents were used as obtained: U (depleted, ORNL),  $\text{Cu}_2\text{S}$  (Alfa, 99.95%),  $\text{BaS}$  (Alfa, 99.7%),  $\text{NaBr}$  (Alfa, 99.99%), S (Aldrich, 99.5%).  $\text{Ba}_2\text{Cu}_2\text{US}_5$  was prepared by a two-step reaction. In the first step, a mixture of 0.3 mmol  $\text{US}_2$  (prepared from the stoichiometric reaction of U and S at

1223 K for 10 days) and 0.1 mmol  $\text{Cu}_2\text{S}$  were ground thoroughly in an Ar-filled glove box, pressed into a pellet, and then loaded into a fused-silica tube. The tube was sealed under a  $10^{-4}$  Torr atmosphere and placed in a computer-controlled furnace. The sample was heated to 1323 K in 60 h, kept at 1323 K for 90 h, and then the furnace was turned off. In the second step, the tube was opened in a glove box and the resultant product was mixed with 0.1 mmol  $\text{BaS}$  and 2.4 mmol  $\text{NaBr}$  (to aid in crystal growth) and reground. The mixture was then loaded into a fused-silica tube. The tube was sealed under a  $10^{-4}$  Torr atmosphere and heated to 1123 K in 60 h, kept at 1123 K for 240 h, slowly cooled at 3 K/h to 853 K, and then the furnace was turned off. After the product was washed with deionized water and dried with acetone, some black needles were found. Analyses of these needles with an EDX-equipped Hitachi S-3500 SEM showed the presence of Ba, Cu, U, and S. There was no indication of the presence of Na or Br. The compound is moderately stable in air.

A powder phase of  $\text{Ba}_2\text{Cu}_2\text{US}_5$  was then obtained from the stoichiometric reaction of  $\text{BaS}$ ,  $\text{Cu}_2\text{S}$ , and  $\text{US}_2$  in a molar ratio of 2:1:1. The reactants were ground in a glove box and then loaded into a carbon-coated fused-silica tube. The tube was sealed under a  $10^{-4}$  Torr atmosphere and then placed in a computer-controlled furnace where it was heated to 1323 K at 50 K/h and held there for 5 days, and then the furnace was quickly cooled to 293 K at 100 K/h.

\*Corresponding author. Fax: +1 847 491 2976.

E-mail address: [ibers@chem.northwestern.edu](mailto:ibers@chem.northwestern.edu) (J.A. Ibers).

X-ray powder diffraction analysis of the powder was performed at 293 K in the angular range of  $2\theta = 10\text{--}70^\circ$  (CuK $\alpha$  radiation,  $\lambda = 1.5418 \text{ \AA}$ ) with a step scan width of  $0.02^\circ$  and a fixed counting time of 3 s/step. The experimental diffraction pattern of the sample was in agreement with that calculated from the single-crystal data. No obvious impurity could be found in the pattern.

## 2.2. Structure determination

Single-crystal X-ray diffraction data were collected with the use of graphite-monochromatized MoK $\alpha$  radiation ( $\lambda = 0.71073 \text{ \AA}$ ) at 153 K on a Bruker Smart-1000 CCD diffractometer [21]. The crystal-to-detector distance was 5.023 cm. Crystal decay was monitored by re-collecting 50 initial frames at the end of data collection. Data were collected by a scan of  $0.3^\circ$  in  $\omega$  in groups of 606, 606, 606, and 606 frames at  $\phi$  settings of  $0^\circ$ ,  $90^\circ$ ,  $180^\circ$ , and  $270^\circ$  with an exposure time of 15 s/frame. The collection of the intensity data was carried out with the program SMART [21]. Cell refinement and data reduction were carried out with the use of the program SAINT [21], and a face-indexed absorption correction was performed numerically with the use of the program XPREP [22]. Then the program SADABS [21] was employed to make incident beam and decay corrections.

The structure was solved with the direct-methods program SHELXS and refined with the least-squares program SHELXL of the SHELXTL suite of programs [22]. The final refinement included anisotropic displacement parameters and a secondary extinction correction. The program TIDY [23] was then employed to standardize the atomic coordinates. Additional experimental details are given in Table 1 and in ‘‘Supporting material’’. Selected metrical details are presented in Table 2.

## 2.3. Magnetic susceptibility measurement

Magnetic susceptibility as a function of temperature was measured on an 11.3 mg powder sample of Ba<sub>2</sub>Cu<sub>2</sub>US<sub>5</sub> with the use of a Quantum Design SQUID magnetometer (MPMS5 Quantum Design). The sample was loaded into a gelatin capsule. Both zero-field cooled (ZFC) and field-cooled (FC) susceptibility data were collected between 2 and 300 K at applied fields of both 1000 and 2000 G. The susceptibility data in the temperature range 180–300 K were fit by a least-squares procedure to the Curie–Weiss equation  $\chi = C/(T - \theta_p)$ , where  $C$  is the Curie constant and  $\theta_p$  is the Weiss constant. The effective moment ( $\mu_{\text{eff}}$ ) was calculated from the equation  $\mu_{\text{eff}} = (7.997C)^{1/2} \mu_B$  [24].

## 3. Results and discussion

### 3.1. Synthesis

A two-step reaction afforded a few black crystals of Ba<sub>2</sub>Cu<sub>2</sub>US<sub>5</sub>. In the first step, US<sub>2</sub> and Cu<sub>2</sub>S were reacted at

Table 1  
Crystal data and structure refinement for Ba<sub>2</sub>Cu<sub>2</sub>US<sub>5</sub>

fw	800.09
Space group	<i>C2/m</i>
<i>Z</i>	2
<i>a</i> (Å)	13.606(3)
<i>b</i> (Å)	4.0825(8)
<i>c</i> (Å)	9.3217(19)
$\beta$ (°)	116.32(3)
<i>V</i> (Å <sup>3</sup> )	464.11(16)
<i>T</i> (K)	153(2)
$\lambda$ (Å)	0.71073
$\rho_c$ (g cm <sup>−3</sup> )	5.725
$\mu$ (cm <sup>−1</sup> )	312.94
<i>R</i> ( <i>F</i> ) <sup>a</sup>	0.0228
<i>R</i> <sub>w</sub> ( <i>F</i> <sub>o</sub> ) <sup>b</sup>	0.0572

<sup>a</sup>  $R(F) = \sum ||F_o| - |F_c|| / \sum |F_o|$  for  $F_o^2 > 2\sigma(F_o^2)$ .

<sup>b</sup>  $R_w(F_o^2) = \{\sum [w(F_o^2 - F_c^2)^2] / \sum F_o^4\}^{1/2}$  for all data.  $w^{-1} = \sigma^2(F_o^2) + (0.03P)^2$ , where  $P = (F_o^2 + 2F_c^2)/3$  for  $F_o^2 > 0$ ;  $w^{-1} = \sigma^2(F_o^2)$  for  $F_o^2 \leq 0$ .

Table 2  
Selected interatomic distances (Å) and angles (°) for Ba<sub>2</sub>Cu<sub>2</sub>US<sub>5</sub>

Ba–S1 × 2	3.180(2)
Ba–S1	3.496(2)
Ba–S2	3.322(2)
Ba–S2 × 2	3.393(2)
Ba–S3 × 2	3.067(1)
U–S1 × 2	2.673(2)
U–S2 × 4	2.770(1)
Cu–S1 × 2	2.381(1)
Cu–S2	2.368(2)
Cu–S3	2.305(1)
S1–U–S1	180
S1–U–S2	89.87(5)
S2–U–S2	180
S2–U–S2	85.07(6)
S1–Cu–S1	118.01(9)
S1–Cu–S2	108.11(6)
S1–Cu–S3	109.07(5)
S2–Cu–S3	103.49(6)

1323 K. In the second step, the product of the first step was ground with BaS and NaBr (to aid in crystal growth) and the reaction was carried out at 1123 K. A rational stoichiometric synthesis involving BaS, Cu<sub>2</sub>S, and US<sub>2</sub> at 1323 K in a molar ratio of 2:1:1 afforded a pure powder phase but no single crystals.

### 3.2. Structure

Ba<sub>2</sub>Cu<sub>2</sub>US<sub>5</sub> crystallizes in a new structure type. In the asymmetric unit, there is one crystallographically unique Ba atom at a site with *m* symmetry, one unique Cu atom at a site with *m* symmetry, and one unique U atom at a site with *2/m* symmetry. The structure consists of  $\frac{2}{\infty} [\text{Cu}_2\text{US}_5^{4-}]$  layers separated by Ba atoms in bicapped trigonal-prismatic coordination (Fig. 1). The two-dimensional  $\frac{2}{\infty} [\text{Cu}_2\text{US}_5^{4-}]$  layer is built from US<sub>6</sub> octahedra and CuS<sub>4</sub>

tetrahedra (Fig. 2). The edge-sharing  $US_6$  octahedra form one-dimensional  ${}^1_{\infty}[US_4^{4-}]$  chains along the [010] direction. A pair of  $CuS_4$  tetrahedra are connected by corner sharing, forming a double  $Cu_2S_7$  unit with a linear Cu–S–Cu arrangement. These double units are connected into a  ${}^1_{\infty}[Cu_2S_5^{8-}]$  chain along the [010] direction by corner sharing. The  ${}^1_{\infty}[US_4^{4-}]$  and  ${}^1_{\infty}[Cu_2S_5^{8-}]$  chains are further connected by edge sharing to form the  ${}^2_{\infty}[Cu_2US_5^{4-}]$  layer. The connectivity of the  $MS_n$  polyhedra in the [001] direction of the layer is *oct tet tet oct tet tet*. This connectivity is similar to that in the  ${}^2_{\infty}[Cu_2ZrS_4^{2-}]$  layer in  $Na_2Cu_2ZrS_4$  [25]. However, in  $Na_2Cu_2ZrS_4$  the  $CuS_4$  tetrahedra are connected to each other by both corner sharing and edge sharing, whereas in  $Ba_2Cu_2US_5$  the  $CuS_4$  tetrahedra are connected to each other only by corner sharing.

The shortest S...S distance is 3.670(2) Å. Thus, there are no S–S bonds and formal oxidation states of 2+, 4+, 1+, and 2– may be assigned to Ba, U, Cu, and S, respectively. In this way charge balance is achieved.

Selected bond distances are listed in Table 2. The U–S distances, which range from 2.673(2) to 2.770(1) Å, are similar to those in other  $U^{4+}$  sulfides, for example  $BaUS_3$  (2.680(5)–2.709(5) Å) [15,16]; the Cu–S distances range from 2.305(1) to 2.381(1) Å, consistent with those of 2.3386(9)–2.3464(8) Å in  $KY_2CuS_4$  [26]; and the Ba–S distances range from 3.0673(8) to 3.496(2) Å, comparable to those of 3.118(2)–3.230(1) Å in  $BaLaCuS_3$  [27].

### 3.3. Magnetism

The inverse molar magnetic susceptibility  $1/\chi_m$  as a function of temperature for  $Ba_2Cu_2US_5$  is shown in Fig. 3. The ZFC and FC data are essentially superimposable. The plot of  $1/\chi_m$  vs.  $T$  has a continually changing slope, especially at low temperatures. There is no obvious

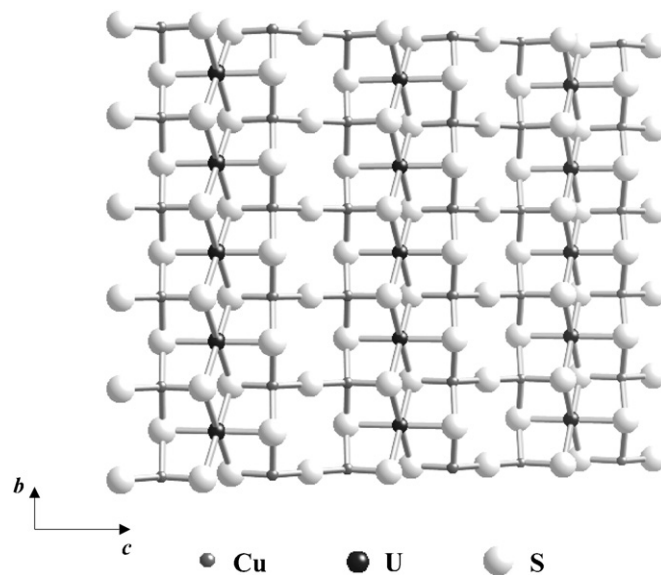


Fig. 2. The  ${}^2_{\infty}[Cu_2US_5^{4-}]$  layer in  $Ba_2Cu_2US_5$ .

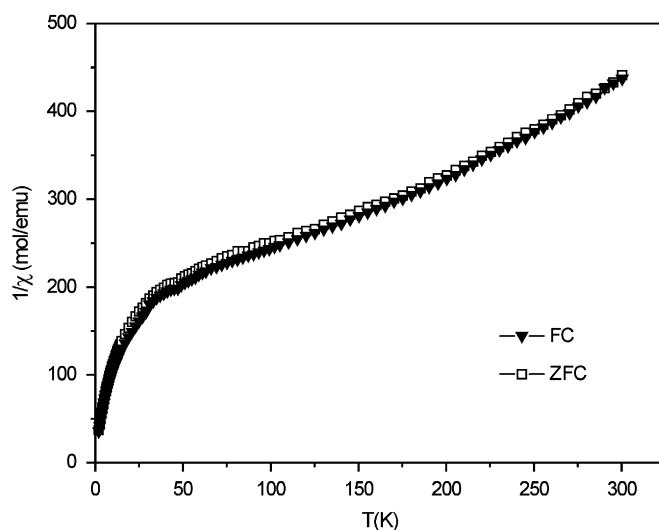


Fig. 3.  $1/\chi_m$  (ZFC and FC) vs.  $T$  for  $Ba_2Cu_2US_5$ , in an applied field of 1000 G.

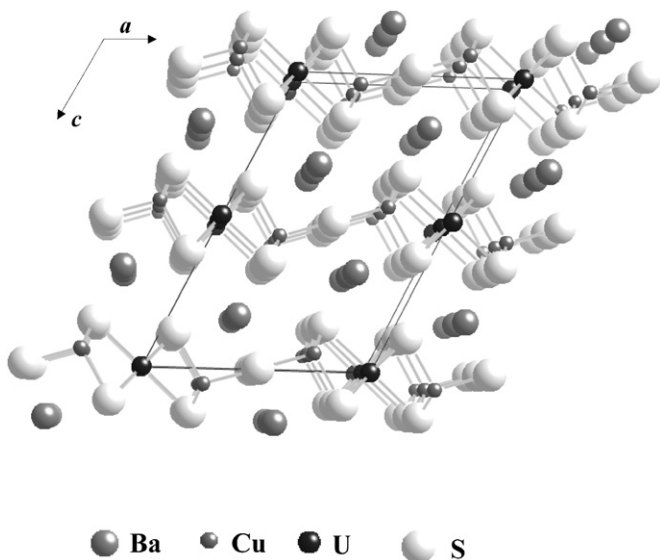


Fig. 1. Unit cell of  $Ba_2Cu_2US_5$  viewed down [010].

magnetic ordering. For  $T > 180$  K, the data can be fit to the Curie–Weiss law  $\chi_m^{-1} = (T - \theta_p)/C$ , although such an approach is not without its pitfalls [28]. The values of the Curie constant  $C$ , the Weiss constant  $\theta_p$ , and the effective magnetic moment  $\mu_{\text{eff}}$  are 0.907(2) emu K mol $^{-1}$ ,  $-92.9(4)$  K, and 2.69(2)  $\mu_B/U$ , respectively. The value of  $\mu_{\text{eff}}$  is smaller than the theoretical one for  $U^{4+}$  (3.58  $\mu_B$ ) [29]. However, it is comparable to the value of 2.5  $\mu_B/U$  for  $Cu_2U_3S_7$  [30]. The value of  $\theta_p$  may indicate local antiferromagnetic ordering. The rapidly changing slope of the data at low temperatures possibly results from crystal field effects. Because of the diffuse nature of the 5f electrons,  $U^{4+}$  exhibits pronounced crystal-field effects in some paramagnetic salts with small  $\mu_{\text{eff}}$  values (2.60–2.91  $\mu_B$ ) [31].

## Supporting material

The crystallographic file in cif format for Ba<sub>2</sub>Cu<sub>2</sub>US<sub>5</sub> has been deposited with FIZ Karlsruhe as CSD number 418464. These data may be obtained free of charge by contacting FIZ Karlsruhe at +49 7247 808 666 (fax) or [crysdata@fiz-karlsruhe.de](mailto:crysdata@fiz-karlsruhe.de) (e-mail).

## Acknowledgments

This research was supported by the US Department of Energy BES Grant ER-15522. This work made use of facilities supported by the MRSEC program of the National Science Foundation (DMR05-20513) at the Materials Research Center of Northwestern University.

## References

- [1] J.A. Cody, J.A. Ibers, *Inorg. Chem.* 34 (1995) 3165–3172.
- [2] A.C. Sutorik, M.G. Kanatzidis, *Chem. Mater.* 9 (1997) 387–398.
- [3] K.-S. Choi, R. Patschke, S.J.L. Billinge, M.J. Waner, M. Dantus, M.G. Kanatzidis, *J. Am. Chem. Soc.* 120 (1998) 10706–10714.
- [4] B.C. Chan, Z. Hulvey, K.D. Abney, P.K. Dorhout, *Inorg. Chem.* 43 (2004) 2453–2455.
- [5] H. Mizoguchi, D. Gray, F.Q. Huang, J.A. Ibers, *Inorg. Chem.* 45 (2006) 3307–3311.
- [6] A.A. Narducci, J.A. Ibers, *Inorg. Chem.* 39 (2000) 688–691.
- [7] K. Chondroudis, M.G. Kanatzidis, *J. Am. Chem. Soc.* 119 (1997) 2574–2575.
- [8] K.-S. Choi, M.G. Kanatzidis, *Chem. Mater.* 11 (1999) 2613–2618.
- [9] R.H. Hess, P.L. Gordon, C.D. Tait, K.D. Abney, P.K. Dorhout, *J. Am. Chem. Soc.* 124 (2002) 1327–1333.
- [10] K. Chondroudis, M.G. Kanatzidis, *C. R. Acad. Sci. Paris* 322 (1996) 887–894.
- [11] A.C. Sutorik, R. Patschke, J. Schindler, C.R. Kannewurf, M.G. Kanatzidis, *Chem. Eur. J.* 6 (2000) 1601–1607.
- [12] D.L. Gray, L.A. Backus, H.-A. Krug von Nidda, S. Skanthakumar, A. Loidl, L. Soderholm, J.A. Ibers, *Inorg. Chem.* 46 (2007) 6992–6996.
- [13] S.A. Sunshine, D. Kang, J.A. Ibers, *J. Am. Chem. Soc.* 109 (1987) 6202–6204.
- [14] M. Komac, L. Golic, D. Kolar, B.S. Brcic, *J. Less-Common Met.* 24 (1971) 121–128.
- [15] R. Brochu, J. Padiou, D. Grandjean, *C.R. Seances, Acad. Sci., Ser. C* 271 (1970) 642–643.
- [16] R. Lelieveld, D.J.W. IJdo, *Acta Crystallogr. Sect. B: Struct. Crystallogr. Cryst. Chem.* 36 (1980) 2223–2226.
- [17] R. Brochu, J. Padiou, J. Prigent, *C.R. Seances, Acad. Sci., Ser. C* 274 (1972) 959–961.
- [18] R. Brochu, J. Padiou, J. Prigent, *C. R. Acad. Sci. Paris* 270 (1970) 809–810.
- [19] M. Potel, R. Brochu, J. Padiou, *Mater. Res. Bull.* 10 (1975) 205–208.
- [20] A.A. Narducci, J.A. Ibers, *Inorg. Chem.* 37 (1998) 3798–3801.
- [21] Bruker, SMART Version 5.054 Data Collection and SAINT-Plus Version 6.45a Data Processing Software for the SMART System, Bruker Analytical X-ray Instruments, Inc., Madison, WI, USA, 2003.
- [22] G.M. Sheldrick, SHELXTL Version 6.14, Bruker Analytical X-ray Instruments, Inc., Madison, WI, USA, 2003.
- [23] L.M. Gelato, E. Parthé, *J. Appl. Crystallogr.* 20 (1987) 139–143.
- [24] C.J. O'Connor, *Prog. Inorg. Chem.* 29 (1982) 203–283.
- [25] M.F. Mansuetto, J.A. Ibers, *J. Solid State Chem.* 117 (1995) 30–33.
- [26] J. Yao, B. Deng, D.E. Ellis, J.A. Ibers, *J. Solid State Chem.* 176 (2003) 5–12.
- [27] A.E. Christuk, P. Wu, J.A. Ibers, *J. Solid State Chem.* 110 (1994) 330–336.
- [28] S. Hatscher, H. Schilder, H. Lueken, W. Urland, *Pure Appl. Chem.* 77 (2005) 497–511.
- [29] N.N. Greenwood, A. Earnshaw, *Chemistry of the Elements*, Pergamon Press, New York, 1989.
- [30] A. Daoudi, M. Lamire, J.C. Levet, H. Noël, *J. Solid State Chem.* 123 (1996) 331–336.
- [31] P. Gans, J. Marriage, *J. Chem. Soc., Dalton Trans.* 1 (1972) 46–48.